Molecular Crystals and Liquid Crystals
Publication details, including instructions for authors and subscription information:
http://www.tandfonline.com/loi/gmcl16

The Mechanisms of the Polymerization Reactions in Diacetylene Crystals: Esr-Analysis of the Paramagnetic Reaction Imtermediates

Hans Sixl [a] & Werner Neumann [a]

[a] Physikalisches Institut, Teil 3, Universität Stuttgart, D-7000 Stuttgart 80, West Germany

To cite this article: Hans Sixl & Werner Neumann (1984): The Mechanisms of the Polymerization Reactions in Diacetylene Crystals: Esr-Analysis of the Paramagnetic Reaction Imtermediates, Molecular Crystals and Liquid Crystals, 105:1, 41-54

To link to this article: http://dx.doi.org/10.1080/00268948408071641

Mol. Cryst. Liq. Cryst. 1984, Vol. 105, pp. 41-54
0026-8941/84/1054-0041/$18.50/0

THE MECHANISMS OF THE POLYMERIZATION REACTIONS IN DIACETYLENE CRYSTALS: ESR-ANALYSIS OF THE PARAMAGNETIC REACTION INTERMEDIATES

HANS SIXL AND WERNER NEUMANN
Physikalisches Institut, Teil 3, Universität
Stuttgart, D-7000 Stuttgart 80, West Germany

Abstract The mechanisms of the solid state polymerization reactions in diacetylene crystals have been investigated by ESR-spectroscopy. The electronic structure of the diradical, carbene and dicarbene intermediates of the low-temperature photopolymerization reaction of diacetylene crystals have been analyzed. From the chain-lengths dependent ESR fine structure and from the isotropic hyperfine structure detailed information concerning the radical and carbene wavefunctions were deduced. A multiplicity change from S=1 to S=2 occurs at the hexamer intermediates.

INTRODUCTION

During the solid state polymerization reaction monomer crystals of disubstituted diacetylenes ($R-C\equiv C-C\equiv C-R$) are converted to highly perfect polymer crystals[1,2]. The primary photochemical processes occuring in the course of the low-temperature photopolymerization reaction have been investigated very recently by ESR[3-5] and optical absorption spectroscopy[6,7]. They are characterized by the photoinitiation, the chain propagation and the chain termination reactions.

A simple reaction scheme is shown in Figure 1. Upon UV-irradiation into the monomer absorption band in a first step dimer diradical molecules are generated. In successive reaction steps further monomer molecules are added thermally (upon annealing at about 100 K) or optically (upon direct photoexcitation of the adjacent monomer molecules). In the chain termination reactions (not shown in the figure) the reactive chain ends are transformed into unreactive configurations by removal of the radical electrons.

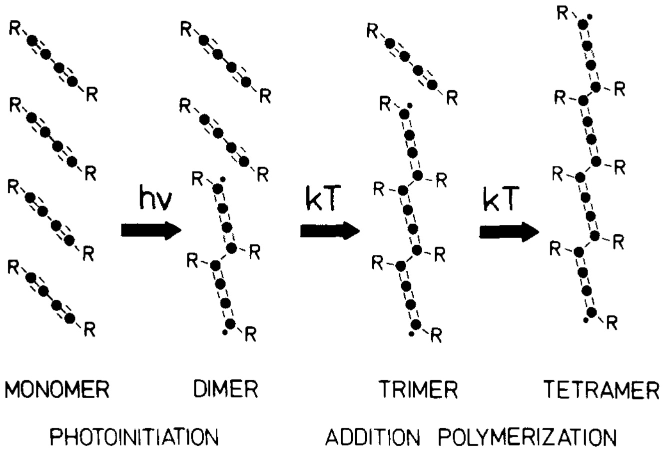

FIGURE 1. Low-temperature polymerization reaction of diacetylene crystals.

The reaction intermediates of this extraordinary solid state reaction have been correlated to dimer, trimer, tetramer molecules etc. with different chemical structures. The physical properties of the reactive short chain intermediates are best characterized by the approximate structures represented in Figure 2. These structures give the principal contributions to the real structures of the DR_n, DC_n and AC_n intermediates. The length of the oligomer molecules is determined by the number n of monomer units. The diradical (DR_n) with $2 \leq n \leq 5$ and the dicarbenes (DC_n) with $n \geq 8$ show a symmetric configuration. The mesomeric butatriene and acetylene structures are expected to be mixed. However at short chain lengths only diradicals are observed. At the other side at long chain length only dicarbenes are present.

In order to obtain a deeper insight into the reaction mechanisms of the polymerization reaction and to elucidate the real electronic structures of the AC_n, DR_n and DC_n intermediates as well as the transformation of the DR intermediates into the DC intermediates at n=6, we have performed a careful ESR study of the fine structure and hyperfine structure of the individual intermediate states. We will show that the change of the DR_n intermediates to the DC_n intermediates is continuous. In the carbene-like configurations of the AC and DC states the p_z electron is delocalized over about two monomer units at the chain ends, mixing carbene configurations with diradical configurations.

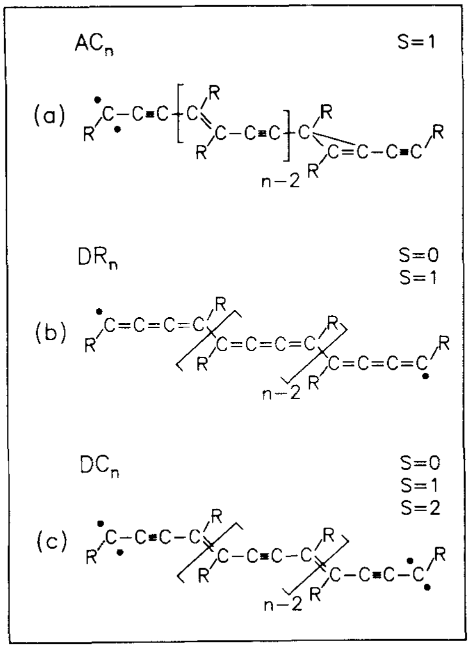

AC_n:

asymmetric carbenes

DR_n:

diradicals

DC_n:

dicarbenes

FIGURE 2. Paramagnetic reaction intermediates of the solid state polymerization reaction. S=0,1,2 are the spin quantum numbers, corresponding to singlet, triplet and quintet states.

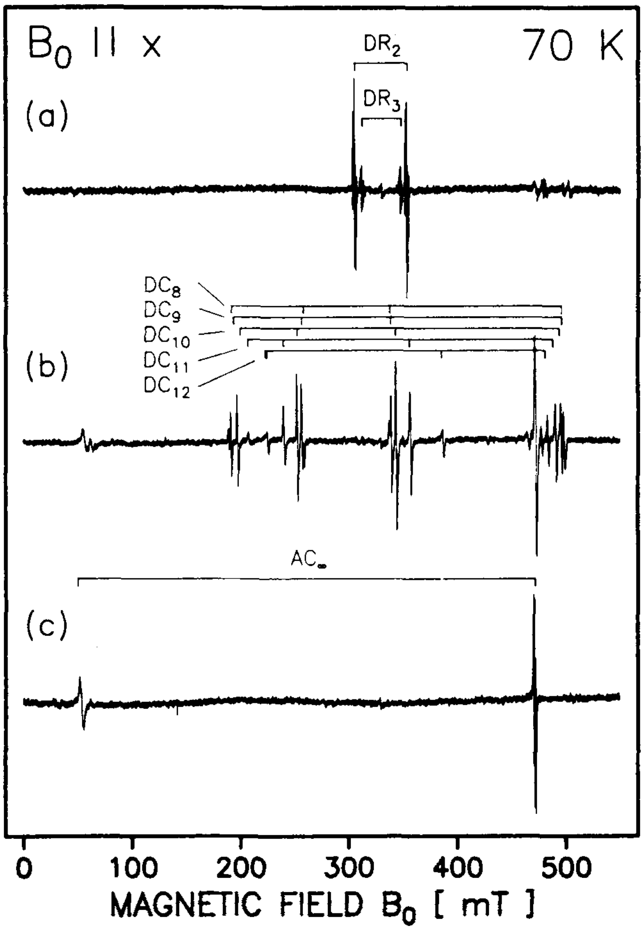

FIGURE 3. ESR-spectra of the paramagnetic reaction intermediates of the low-temperature photoreaction in diacetylene crystals.
(a) after UV-irradiation
(b) and (c) after thermal annealing at T=100 K.
AC_∞ refers to long-chain asymmetric carbene molecules with $n \gtrsim 20$.

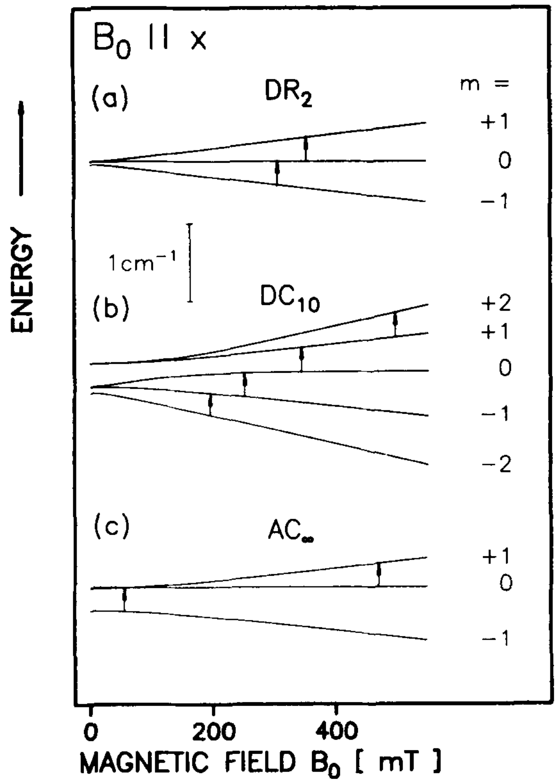

FIGURE 4. Energy level splitting in a magnetic field B_0 parallel to the x-axis of the fine structure tensor. The ESR transitions correspond to the ESR spectra of Figure 3. The following fine structure parameters are used in the calculation.
DR: $D/hc=0.0393\ cm^{-1}$, $E/hc=-0.0016\ cm^{-1}$,
AC: $D/hc=0.2954\ cm^{-1}$, $E/hc=-0.0060\ cm^{-1}$,
DC: $D/hc=0.2960\ cm^{-1}$, $E/hc=-0.0040\ cm^{-1}$.
The D values of the DC states refer to the triplet carbene ends. The singlet-quintet energy separation, which enters into the calculation[8], is $E_{SQ}/hc=4.5\ cm^{-1}$. The energy scale of the Figure is determined by the arrows, indicating the ESR transitions. The lengths of the arrows is given by $0.314\ cm^{-1}$, corresponding to a microwave frequency of 9.30 GHz.

EXPERIMENTAL RESULTS

Fine Structure

Typical ESR spectra of the reaction intermediates of the low-temperature photopolymerization reaction are shown in Figure 3. The spectra (a), (b) and (c) only show a selection of the numerous intermediates observed after UV- irradiation (308 nm) with an excimer laser (a) and after thermal annealing (b) and (c) of the diacetylene monomer crystal. Three types of intermediates can be distinguished. The DR triplet states (a), which show a small fine structure splitting between the two Δm=1 ESR lines, the AC triplet states (c), which show a large fine structure splitting between the two Δm=1 ESR lines and the DC quintet states (b), which also show a large fine structure splitting between the four Δm=1 ESR lines. The triplet states arise from two, the quintet states from four S=1/2 unpaired electrons.

The ESR spectra are described by the spin Hamiltonian

$$\underset{\wedge}{H} = \underset{\wedge}{H}_Z + \underset{\wedge}{H}_{FS} + \underset{\wedge}{H}_{HFS} \qquad (1)$$

$\underset{\wedge}{H}_Z$ is the Hamiltonian of the Zeeman effect

$$\underset{\wedge}{H}_Z = g\mu_B \vec{B}_o \underset{\wedge}{\vec{S}} \qquad (2)$$

with external magnetic field B_o, the g-factor g= 2.0023 and Bohr's magneton μ_B. $\underset{\sim}{\vec{S}}$ is the spin operator with S=1 (triplet) or S=2 (quintet) and the components $\underset{\sim}{S}_x$, $\underset{\sim}{S}_y$ and $\underset{\sim}{S}_z$.

$\underset{\wedge}{H}_{FS}$ is the fine structure Hamiltonian

$$\underset{\wedge}{H}_{FS} = D\underset{\wedge}{S}_z^2 + E(\underset{\wedge}{S}_x^2 - \underset{\wedge}{S}_y^2) \qquad (3)$$

with fine structure parameters D and E.

The energy level splitting and the corresponding ESR-transitions of the DR and AC triplet and DC quintet states are calculated using the Zeeman and the fine structure spin Hamiltonians (2) and (3). The result is shown in Figure 4, which corresponds to the spectra of Figure 3.

ESR Hyperfine Structure

All ESR lines show partially resolved hyperfine structure as shown in Figure 5, due to hyperfine interaction of the electron spin with the nuclear spins $I_1 = I_2 = 1/2$ of the two protons of the CH_2-rest group. In the case of the diradicals and dicarbenes two CH_2 groups of the two chain ends are involved in the hyperfine interaction. In the case of the asymmetric carbenes only one chain end is involved. The experimental hyperfine pattern is reproduced by a computer calculation. The hyperfine splitting of the ESR spectra is almost isotropic, therefore the Hamiltonian of the hyperfine interaction writes

$$\underset{\wedge}{H}_{HFS} = \underset{\wedge}{\vec{S}}\;\underset{\approx}{A}\;\underset{\wedge}{\vec{I}} \approx A\underset{\wedge}{\vec{S}}\underset{\wedge}{\vec{I}} = A_1\underset{\wedge}{\vec{S}}\underset{\wedge}{\vec{I}}_1 + A_2\underset{\wedge}{\vec{S}}\underset{\wedge}{\vec{I}}_2 \qquad (4)$$

A_1 and A_2 are the isotropic hyperfine constants of the two protons of the CH_2 group.

Chain-Lengths Dependences

The fine structure constant D is very sensitive to the shape and extension of the electron wavefunction of the triplet resp. quintet electrons. The isotorpic hyperfine constant A is essentially determined by the spin density at the CH_2 protons. Therefore from both, the fine structure and the hyperfine structure, we are able to deduce the wavefunctions of the different DR_n, DC_n and AC_n intermediates.

The fine structure constants D of the triplet diradical centers as a function of the chain-length n are shown in Figure 6. The D-values of the first four DR triplet states are very small corresponding to the diradical structure of Figure 2. However, between n=5 and 6 there is a remarkable increase of the D-values, which at n=7 almost reaches the limiting D-values of the dicarbene states and of the AC intermediates as shown below.

The hyperfine splitting is given by the interaction of the electron spin with two CH_2 groups. The dependence of the hyperfine constant A_1 obtained from the computer simulation as a function of the chain-length is also shown in Figure 6.

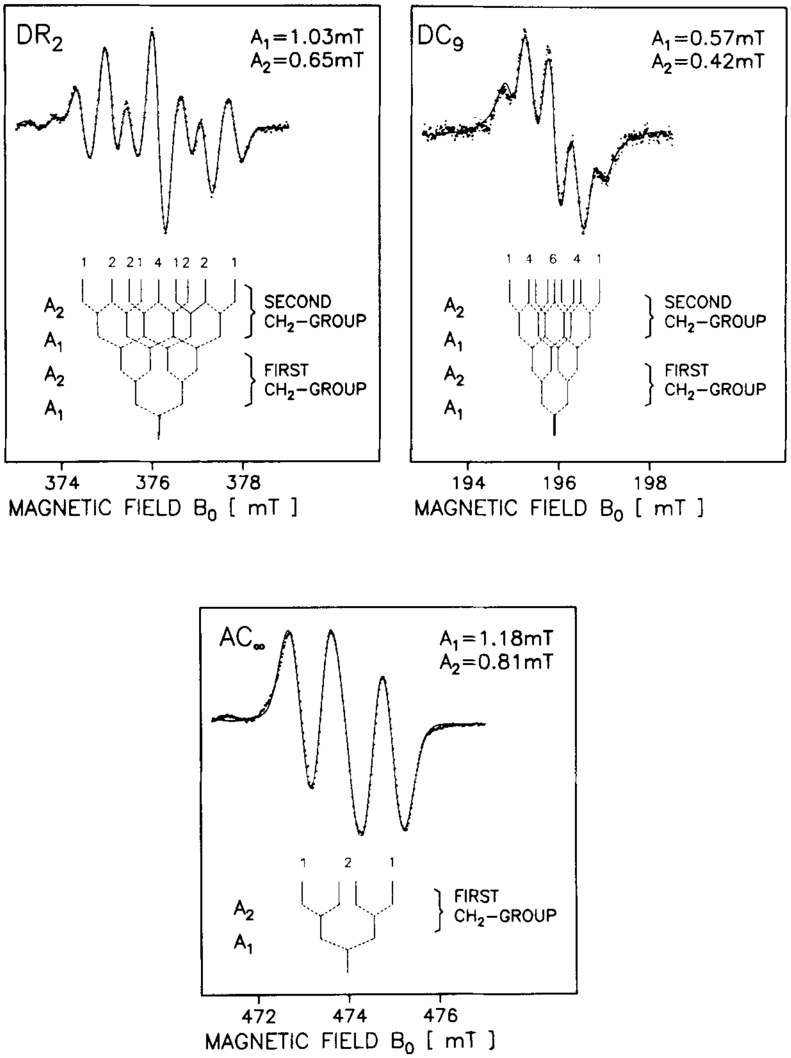

FIGURE 5. Hyperfine structure pattern of the paramagnetic reaction intermediates. The computer simulation has been fitted to the experimental points.

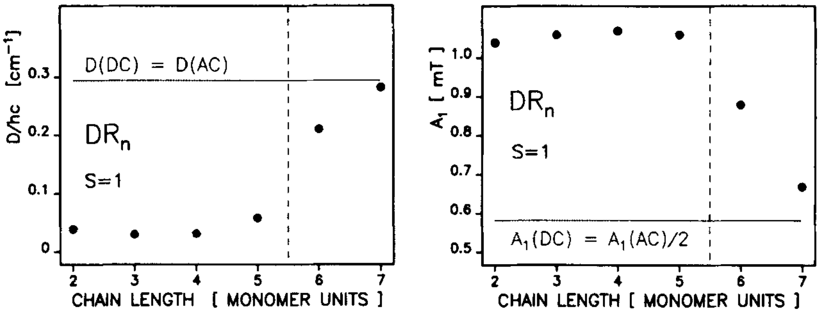

FIGURE 6. Fine structure constants and hyperfine structure constants of the DR_n states as a function of the chain-length n. The dashed line separates the almost pure diradical states with $n \leq 5$ from the mixed states with n=6 and 7.

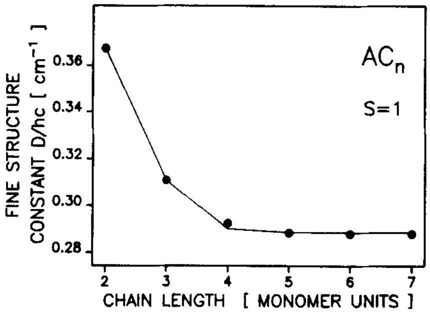

FIGURE 7. Fine structure constants D of the AC_n states as a function of the chain-length n. The points are deduced from the ESR-spectra[4], the curve is calculated[13] using the configuration of Figure 8.

Similar to the behaviour of the D-values, the hyperfine constant is almost constant up to n=5 and drops at n=6 and n=7 down to almost the A_1 value of the dicarbene and to the corresponding value of the AC states.

The fine structure constants D of the triplet asymmetric carbene centers as a function of the chain-length n are shown in Figure 7. The D values of the short chains are essentially larger than those of the long chains. The asymptotic dependence converges very rapidly at n=5 to the final D(∞) value, which is almost identical to that of the triplet carbene ends of the DC molecules.

DISCUSSION

The Diradicals DR_n

The small fine structure splitting of the intermediates with $n \triangleq 5$ and the hyperfine pattern suggest the diradical structure of the DR triplet electrons shown in Figure 2. The two triplet electrons are given by the sp_2-electrons of the diradical carbon $-\dot{C}=$ at the chain ends. All p_z electrons are bound and thus form a complete butatriene chain structure. The analysis of the fine structure and hyperfine structure data yields carbene admixtures, which are less than 10% for $n \triangleq 5$. Starting at n=6 the DR intermediates are transformed gradually into DC intermediates.

The Dicarbenes DC_n

The long-chain (n>7) dicarbene centers are formed by electrostatic coupling of two triplet carbenes[8]. Therefore the dicarbenes are closely related to the long-chain ($n \triangleq 5$) AC_n centers, which also have the same acetylene chain structure (see Figure 2). This relationship is documented in the same fine structure constants of the corresponding triplet states and in the same hyperfine structure relation $A_1(AC)=2A_1(DC)$, which is valid for all AC_n and DC_n centers at long chain length.

In the ESR-experiments eleven different quintet dicarbene centers have been distinguished, ranging from n=7 to n=17. The small overlap of the carbene wavefunctions located at the two chain ends is documented in the D and A-values, which are independent of the chain length.

The individual carbenes of the dicarbene structure are formed by an sp_2-electron and a p_z-electron. In the short chain diradical structures discussed above the two p_z-electrons form a π-bond, which is disrupted in the dicarbene structure. This π-bond has an energy of about 2.5 eV. The disruption of the π-bond is caused by a respective energy gain, which is obtained due to the change of the high-energetic butatriene to the low-energetic acetylene chain structure[9]. Owing to the delocalization of the p_z-electrons, diradical states with butatriene configurations are expected to mix with the carbene configurations. This will be discussed below. Due to their identical chain structures the chain ends of the DC configurations are identical to the chain ends of the AC configurations. The asymmetric carbene structure therefore represents one half of the DC structure.

The Asymmetric Carbenes AC_n

The hyperfine splitting of the AC intermediates is given by the interaction of the electron spin with only one CH_2 group, showing the typical 1:2:1 intensity pattern of Figure 5, clearly demonstrating that the carbene state is located only at one chain end. The other chain end has been terminated by a chain termination reaction.

The identification of the AC and DC intermediates in terms of pure carbene states is not quite correct. It is obvious from the fine structure constants that the D values of the AC and DC states are located almost exactly half way between the pure carbene and the pure diradical structures. For a pure carbene $-\ddot{C}-$ a D value of 0.7 cm^{-1} has been deduced from ESR measurements[10]. Therefore we have to conclude that about 50% of the wavefunctions are not carbene but diradical wavefunctions as shown in Figures 8a and b. The different diradical wavefunctions arise from the fact that the p_z-electrons can be delocalized over the diacetylene chain. However, the deloca-

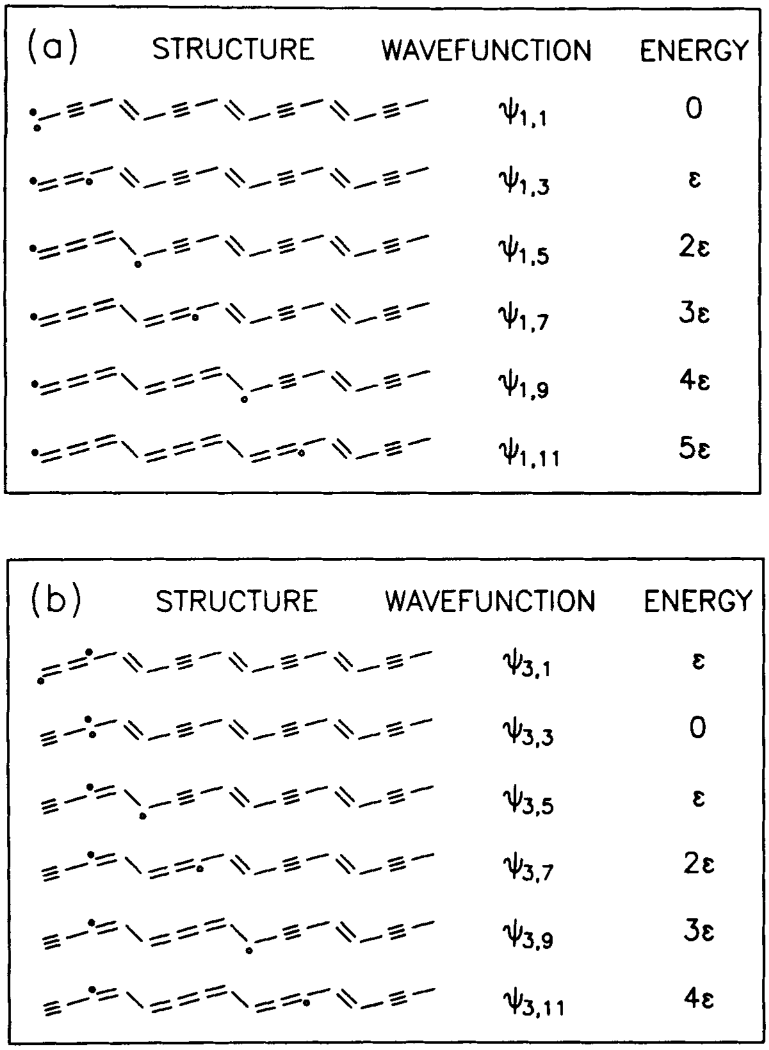

FIGURE 8. Basic configurations of the carbene and diradical states, which form the reactive chain end in the AC and DC intermediates.

lization is restricted to a relatively small distance at the chain ends, due to the non-degeneracy of the butatriene structure and the acetylene structure of the diacetylene chain. The p_z-radical electron in diacetylene chains therefore represents a bond alternation defect similar to that present in cis-polyacetylene chains[11]. In contrast to the p_z-electrons the sp_2-electron can be delocalized only within the first unit cell. The two sets of wavefunctions (a) and (b) correspond to the two possible carbene configurations at the first and third carbon atom. The curve of Figure 7 is the result of a preliminary calculation[13] of the D-values of the short chain AC molecules taking into account the configurations of Figure 8a and b.

CONCLUSIONS

By analysis of the ESR fine and hyperfine structure we have shown that the diradical structure of the short chain intermediates undergoes a transition to the dicarbene structure. From this transition we conclude that the acetylene structure of the oligomer backbone is lower in energy than the butatriene structure. By inspection of the fine structure and hyperfine structure parameters the real electronic structures of the paramagnetic reaction intermediates are deduced[12], which are not perfectly pure diradical or carbene states. Especially the asymmetric carbenes and dicarbenes contain large admixtures of diradical states. The analysis of the ESR-spectra now enables us to calculate the extension of the soliton-like p_z-electron[13]. The knowledge of the electronic structure of the reaction intermediates forms a solid basis for a more complete understanding of reaction mechanisms in the solid state polymerization reaction.

ACKNOWLEDGEMENTS

This work has been supported by the Deutsche Forschungsgemeinschaft. We would like to thank W. Tuffentsammer for crystal preparation.

REFERENCES

1. G. Wegner, Molecular Metals (W.E. Hatfield, Plenum Press, N.Y. 1979) p. 209 and Chemistry and Physics of One-Dimensional Metals (H.J. Keller, Plenum Press, N.Y. 1977) p. 297.
2. R.H. Baughman and R.R. Chance, Synthesis and Properties of Low-Dimensional Materials (J.S. Miller and A. Epstein, Ac. of Science, N.Y. 1978) p. 795, D. Bloor, Developments in Crystalline Polymers (D.C. Basset, Appl. Sci. Publ., London 1982) in press.
3. Y. Hori and L.D. Kispert, J. Chem. Phys. 69, 3826 (1978) and J. Am. Chem. Soc. 101, 3173 (1979).
4. C. Bubeck, H. Sixl and H.C. Wolf, Chem. Phys. 32, 231 (1978), C. Bubeck, W. Neumann and H. Sixl, Chem. Phys. 48, 269 (1980), R.A. Huber, M. Schwoerer, H. Benk and H. Sixl, Chem. Phys. Lett. 78, 303 (1981).
5. W. Neumann and H. Sixl, Chem. Phys. 50, 273 (1980) and 58, 303 (1981).
6. W. Hersel, H. Sixl and G. Wegner, Chem. Phys. Lett. 73, 288 (1980), H. Gross and H. Sixl, Chem. Phys. Lett. 91, 262 (1982), H. Gross and H. Sixl, Mol. Cryst. Liq. Cryst. 93, 261 (1983).
7. H. Niederwald, H. Eichele and M. Schwoerer, Chem. Phys. Lett. 72, 242 (1980), H. Niederwald, K.-H. Richter, W. Güttler and M. Schwoerer, Mol. Cryst. Liq. Cryst. 93, 247 (1983).
8. H. Benk and H. Sixl, Mol. Phys. 42, 779 (1981).
9. J.L. Brêdas, R.R. Chance, R. Silbey, G. Nicolas and Ph. Durand, J. Chem. Phys. 75, 255 (1981).
10. R.A. Bernheim and S.H. Chien, J. Chem. Phys. 65, 2023 (1976).
11. W.P. Su, J.R. Shrieffer and A.J. Heeger, Phys. Rev. B22, 2099 (1980).
12. W. Hartl and M. Schwoerer, Chem. Phys. 69, 443 (1982).
13. W. Neumann and H. Sixl, to be published